Appl. Phys. B 62, 51–57 (1996)

Applied Physics B Lasers and Optics

Comparative study of spectral narrowing of a pulsed Ti:Sapphire laser using pulsed and CW injection seeding

N.J. Vasa[1], M. Tanaka[1], T. Okada[1], M. Maeda[1], O. Uchino[2]

[1] Department of Electrical Engineering, Kyushu University, Hakozaki, Fukuoka 812, Japan
(Fax: + 81-92/631-2790)
[2] Division of Meteorological Satellite and Observation System, Meteorological Research Institute, Tsukuba, Ibaraki 305, Japan

Received : 10 October 1994/Accepted: 12 April 1995

Abstract. We report a comparative study of a pulsed as well as continuous-wave (cw) injection seeding of a Ti : Sapphire laser pumped by a Q-switched frequency-doubled Nd^{3+} : YAG laser for achieving narrow spectral bandwidth. The results have indicated that the Ti : Sapphire laser using either a pulsed or a cw injection seeding could achieve efficient energy extraction in a narrow spectral bandwidth. In the case of pulsed injection seeding, the injection energy required for the complete injection seeding critically depended upon the timing of the Ti : Sapphire laser with respect to the delayed onset of the slave laser. On the other hand, in the case of cw injection seeding, the spectral bandwidth of the Ti : Sapphire laser was efficiently narrowed down to approximately 0.01 cm^{-1} with an injection power of less than 1 mW. In both types of injection seeding, characteristics observed experimentally were compared with those obtained by a numerical simulation code based on the one-dimensional rate-equation model.

PACS: 42.55; 42.60

In recent years single-frequency, pulsed Ti:Sapphire lasers are being used increasingly for various applications related to Differential Absorption Lidar (DIAL) Measurements of atmospheric species, temperature, and pressure which require narrow spectral bandwidth, high beam quality, and tunability [1]. The most traditional method of achieving a narrow spectral bandwidth is simply inserting various dispersive elements like gratings, prisms, etalons, birefringent filters, or their combinations in the laser cavity. As the dispersive elements used for wavelength selection are lossy, laser threshold increases and the slope efficiency of the laser decreases. Also, optical damage to these elements can be a limiting factor to laser performance. One direct technique for achieving narrowband, tunable radiation with high output energy is the laser amplification method. However, it requires multistage amplification to attain highly saturated amplification.

An alternative and more efficient technique for line narrowing of a pulsed laser is injection seeding, which is also referred to as injection locking. In this arrangement, the injection signal from the narrow-band width master laser is injected into a cavity of some high-power laser, which is also referred to as a slave laser, to force the slave laser to oscillate on a narrow spectral bandwidth. As efficient narrowing can be obtained in a low-energy injection, it permits precise frequency control and efficient operation of line narrowing of the slave laser. Although we can use a pulsed or a cw-type master laser, as a result of their different operating conditions, the injection seeding has different requirements to achieve effective spectral narrowing of the Ti : Sapphire slave laser.

Several works have reported on the injection seeding of pulsed Ti : Sapphire lasers [1–5]. Most of them were using a cw diode laser as an injection source, which is convenient for the practical use. But another possibility for the injection source is a tunable pulsed laser, whereby a large injection power as well as a large tuning range can be obtained very easily. In this paper, we made a comparative study of both types of injection seeding to understand their characteristic requirements for achieving higher locking efficiency. A pulsed Ti : Sapphire laser and a predominantly single-mode diode laser was used as an injection source. The experimental results of pulsed and cw injection seeding are discussed in Sects. 1.1 and 1.2, respectively. To understand the experimental results for a comparative study of different types of injection seeding, a theoretical analysis is developed which is described in Section 2. Using spectro-temporal equations, free-running and injection-seeded conditions are simulated. The theoretical analysis has explained various characteristic requirements for different types of injection seeding and the effect on locking efficiency.

1 Experimental

1.1 Pulsed injection seeding

The optical configuration for pulsed injection seeding is shown in Fig. 1. A Q-switched, frequency-doubled,

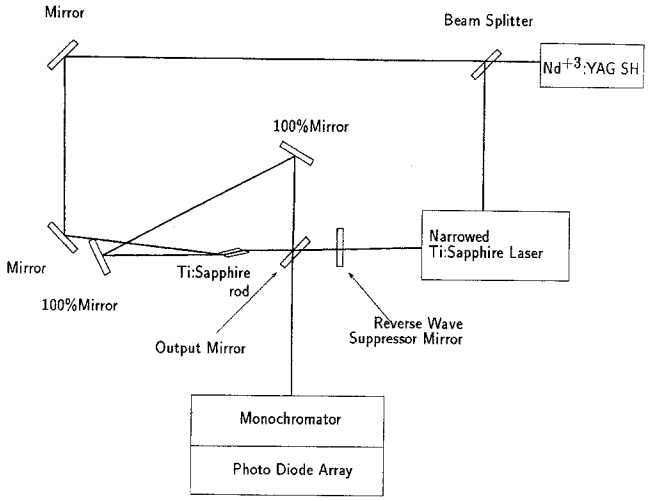

Fig. 1. Optical setup for pulsed injection seeding

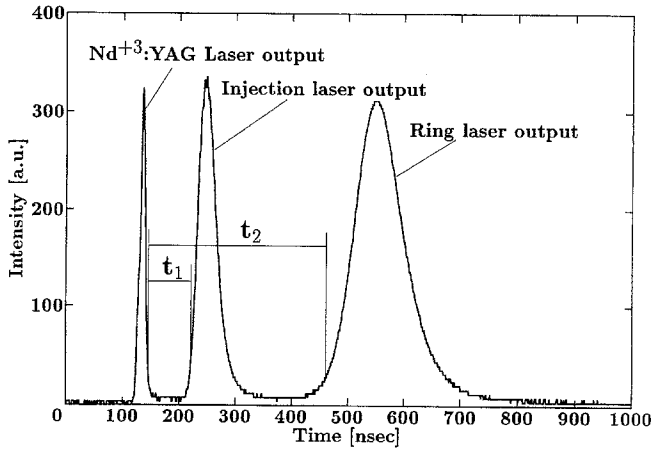

Fig. 2. Measured temporal pulse shapes of pump Nd^{3+}:YAG laser, Ti:Sapphire master laser, and Ti:Sapphire ring slave laser. The delay-ratio parameter can be defined as t_1/t_2

Nd^{3+}:YAG pump laser (Spectra-Physics GCR-3) was used for pumping both master and slave lasers at a repetition rate of 10 Hz. The pulsed master laser, having an output energy of 0.7 mJ at 797.5 nm, had a straight cavity configuration, in which three Brewster prisms and a fine tuning etalon were inserted to obtain a narrow spectral linewidth of approximately 0.15 cm^{-1} [6]. The slave laser resonator consisted of a 1.15 m ring cavity with a flat output coupler having a reflectivity of 0.8 at 780 nm. To achieve a unidirectional operation of the ring resonator, a partially reflecting Reverse-Wave Suppressor Mirror (RWSM) having a reflectivity of 0.55 at 780 nm was placed in the reverse direction output allowing less than 2% of the forward output near threshold [2]. The free-running output of the slave laser was having a broadband spectrum from 800 to 820 nm with an output energy of 5.7 mJ corresponding to a pump energy of 57 mJ. In this experiment, longitudinal mode matching between the pulsed master laser radiation and the free-running slave laser cavity was automatically achieved, because of the wider spectral width of the pulsed master laser as compared to the mode spacing of the slave laser.

In our experiment, two parameters, namely delay ratio and injection energy, were considered for studying their effects on locking efficiency. The delay ratio was defined as a ratio of t_1 and t_2 in Fig. 2, where t_1 is the delay of the master laser and t_2 is that of the slave laser pulse after the pumping. In the measurement of the delay ratio, the time difference was measured at 10% of the peak intensity of the corresponding output pulse as a convention. The delay ratio was changed by controlling the pumping energy of the master laser. As the pumping energy was reduced, the time delay of the master laser was increased. The delay of the pulsed master laser was changed from approximately 20 to 180 ns, and delay ratios from 0.1 to 0.6 were achieved. The injection energy was changed quantitatively without changing its spectral characteristics by using various neutral density filters in the path of injection seeding. The spectral structure of the injection-seeded laser was measured by passing the laser output through an optical fiber into a spectrograph and monitoring

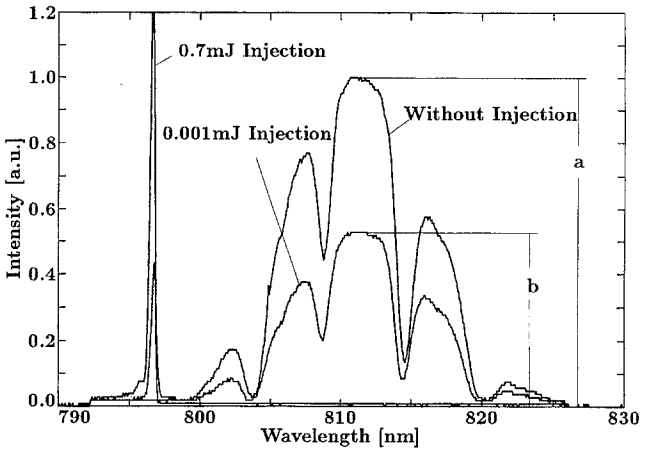

Fig. 3. Spectra of Ti:Sapphire slave laser output with and without injection-seeding operation. Locking efficiency ϕ is defined as $\phi = 1 - b/a$

the signal with a photodiode array (Hamamatsu C4350). Output pulse shapes were measured using a PIN photodiode.

Figure 3 shows spectra of the Ti:Sapphire slave laser output with and without injection seeding. Periodic dips observed in the spectra might have been the effect of the birefringence of the Ti:Sapphire crystal. The output energy of the slave laser was not changed by the injection, which suggested the homogeneous broadening of the Ti:Sapphire spectrum. In order to evaluate the degree of injection seeding, a parameter, the locking efficiency ϕ, was used, which can be defined as the ratio of the lasing energy in the injected mode to the total lasing energy.

In case of homogeneously broadened spectra, this calculation can be further simplified as shown in Fig. 3, since the energy from the quenched mode will be concentrated into the injected mode. Thus, locking efficiency ϕ can be expressed as follows:

$$\phi = 1 - \frac{b}{a}, \tag{1}$$

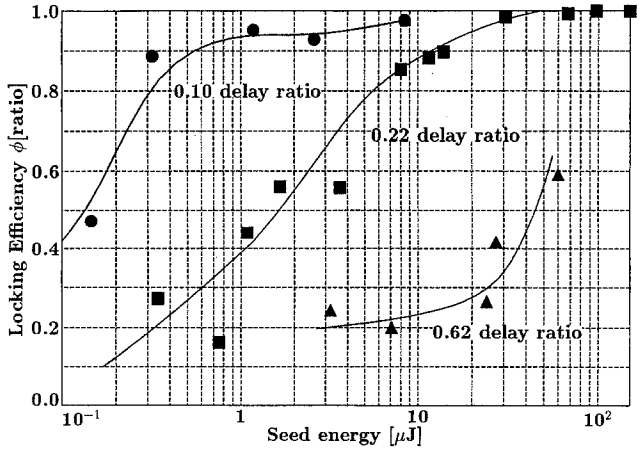

Fig. 4. Effect of pulse delay on locking efficiency

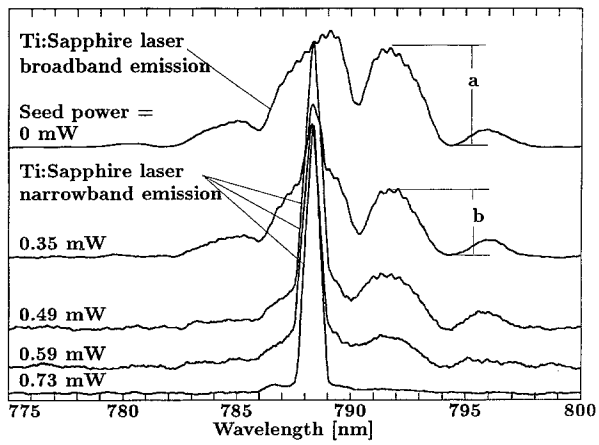

Fig. 6. Spectra of cw injection-seeded Ti:Sapphire slave laser output. Locking efficiency is defined as $\phi = 1 - b/a$

where a is the height of any mode other than the injected mode in the free-running condition, and b is the height of the same mode in the injection seeding.

Figure 4 shows the locking efficiency ϕ as a function of the injection energy for three different delay ratios. It clearly indicates that for a given delay ratio, the locking efficiency ϕ rapidly increased as the injection energy increased. For example, for a delay ratio of 0.22, as the injection energy was increased from 0.18 to 12 μJ, the locking efficiency ϕ had increased from 0.1 to approximately 1 indicating complete injection seeding. Further, the injection energy required for obtaining a given locking efficiency ϕ depended strongly upon the delay ratio. When the delay ratio was decreased from 0.22 to 0.1 in Fig. 4, the injection energy required for achieving $\phi = 90\%$ had reduced from 12 to 0.4 μJ.

1.2 CW injection seeding

The optical setup for cw injection seeding of the Ti:Sapphire laser is shown in Fig. 5. The same pumping configuration was used when applied in pulsed injection seeding.

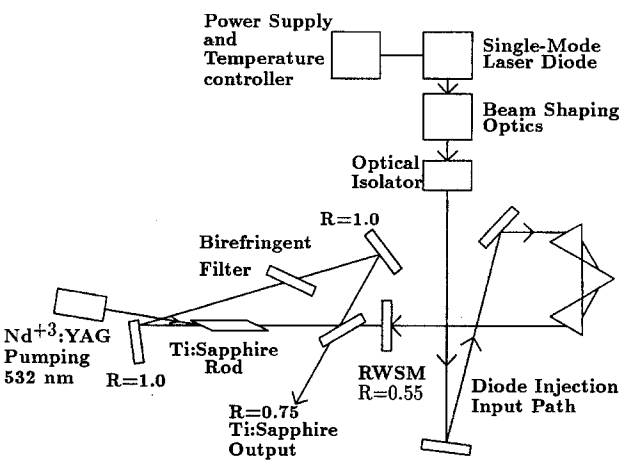

Fig. 5. Optical setup for cw injection seeding

A single-mode laser diode (Sharp LT024PD0) was used as an injection-seed source, which is also referred to as cw master laser. Available output power was 30 mW at a nominal wavelength of 780 nm. The output from the diode laser was injected into the slave laser cavity through collimating optics and an optical isolator. The isolation was of 40 dB at 783 nm within an effective range of 8 nm. A set of three Brewster prisms was also used between the RWSM and the isolator to provide further protection by dispersing the slave laser output. In this experiment, a birefringent filter was used for the coarse control of the slave laser wavelength. The tuning range of the slave laser by this filter was from 770 to 840 nm, with a bandwidth of approximately 15 nm, and the output energy was 2.2 mJ for a pump energy of 35 mJ at a wavelength of 788 nm.

The slave laser spectra was measured for two different cases. In case I, the wavelength of the cw master laser was tuned on the center of the tuning curve of the slave laser, i.e., 788 nm. While in case II, the wavelength of the slave laser was tuned in such a way to obtain comparatively maximum gain at approximately 794 nm and comparatively less gain at 788 nm in the free-running condition. Thus, the injection wavelength of 788 nm was tuned on the wing of the tuning curve of the slave laser. Figure 6 shows the slave laser output spectra with and without injection-seeding operation for case I. The indicated value of the injection power was measured inside the slave laser cavity. When no injection seeding was applied, the spectral output extended from 782 to 798 nm with some modulation due to the birefringence effect of the laser crystal. Subsequently, as the injection power was increased, the broad emission was quenched and the spectral narrowing was achieved. In Fig. 6, the spectral width of the injection-seeded laser is wider than the actual due to a low resolution of the spectrometer.

The locking efficiency ϕ was measured in the same manner as in Sect. 1.1. For example, the bottom spectral scan in Fig. 6 shows that approximately 83% of the energy was extracted in the narrow linewidth. Locking efficiency ϕ obtained from Fig. 6 is plotted as a function of the injection power for both cases in Fig. 7. In case I, the locking efficiency ϕ increased from 0 to

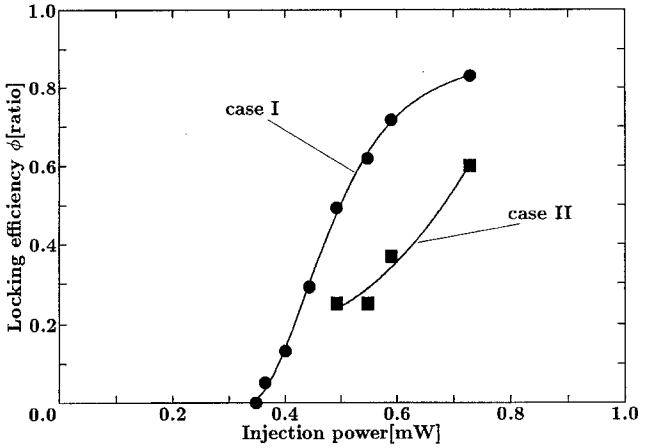

Fig. 7. Locking efficiency with respect to cw injection power for different cases of injection seeding condition. *Case I*: Injection seeding Ti : Sapphire slave laser at the center of the free-running spectra, i.e. at a wavelength of 788 nm. *Case II*: injection seeding Ti : Sapphire slave laser at the wing at a wavelength of 794 nm

approximately 83% when the injection power was increased from 0.35 to 0.73 mW. While case II shows the similar increasing trend but it had achieved approximately 60% locking efficiency for 0.73 mW of the injection power. Thus, in the case of injection seeding at the mode having larger loss, comparatively more injection power was required for achieving the same efficiency as compared to case I.

A Fabry-Perot interferometer (Burleigh RC-140) was used to measure the linewidth. The array detector (Hamamatsu C4350) was used to measure ring fringes of the interferometer through a focusing lens of 1000 mm. The Fabry-Perot interferometer was set for a free-spectral range (FSR) of 0.10 cm^{-1} with a resolution of approximate 0.0024 cm^{-1}. Figure 8 shows interference patterns of (a) the cw master laser, as well as the slave laser (b) without and (c) with injection seeding at an injection power of 0.73 mW. The measured linewidth of the cw master laser was approximately 0.01 cm^{-1}. The measured value of the linewidth of the cw master laser was further confirmed by setting a free-spectral range (FSR) of 0.05 cm^{-1} and extending the resolution to approximately 0.0012 cm^{-1}. Without injection seeding, the slave laser had a broadband output and no visible fringe pattern was obtained as shown in Fig. 8b. Figure 8c shows that with 0.73 mW of the injection-seed power, well-defined fringes with a bandwidth as narrow as the cw master laser. In an improved spatial matching, we obtained similar distinct fringes even with an injection power of 0.58 mW.

2 Theoretical modeling

2.1 Model and formulation

To understand pulsed as well as cw injection seeding in a Ti : Sapphire laser, a computer model for a straight laser cavity is developed [6, 7]. Figure 9 shows the configuration of injection seeding of a laser-cavity model. The analysis is based on a set of coupled rate equations for

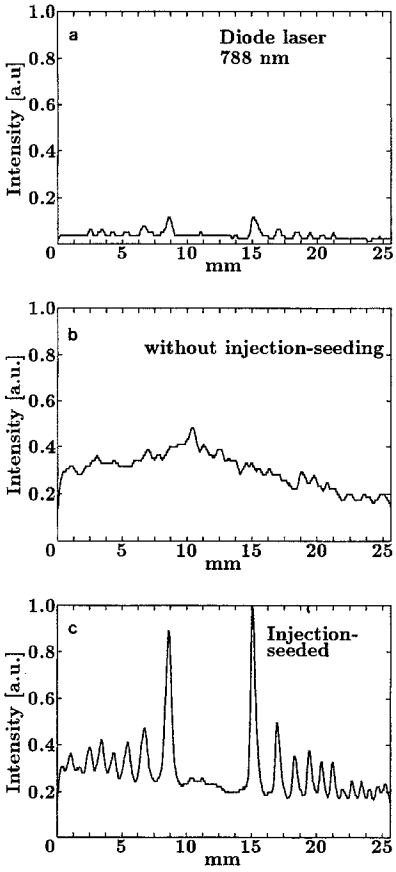

Fig. 8a–c. Fabry-Perot interference fringe. **a** cw injection-seed laser. **b** Free-running condition of the Ti : Sapphire laser. **c** Ti : Sapphire laser with cw injection seeding. The free spectral range was 0.1 cm^{-1}

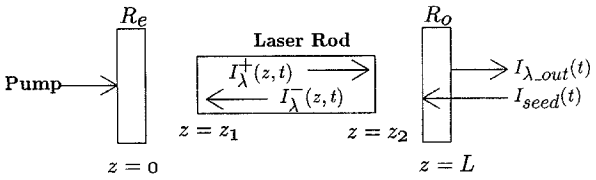

Fig. 9. Configuration of injection-seeded cavity model for numerical simulation

population densities and one-dimensional photon transport equations for photon fluxes.

In order to simplify the computation, we have made the following assumptions:

(*i*) The equations are written for a homogeneously broadened medium so that the same $N_i(x, t)$ $(i = 1, T)$ molecules interact with the radiation at all wavelengths within the fluorescence band.
(*ii*) The upper-state population is calculated at time $t = 0$ and the pumping and the relaxation terms are neglected.
(*iii*) Transverse variation in the intensities and population densities is assumed to be uniform for this model.
(*iv*) $\sigma_e(\lambda)$ values obtained by Eggleston et al. are used for the calculation [8].

Table 1. Numerical values used in the simulation

Symbol	Numerical value
E_{po}	0.09 (J)
S	0.0314 (cm^2)
Length	2 (cm)
α	0.63 (cm^{-1})
τ	3.2×10^{-6} (ns) [9]
η	1.76
$\sigma_e(\lambda)$	Varying as per λ (cm^2) [8]
$E(\lambda)$	Varying as per λ [8]
f	1.0×10^{-14}
R_e	0.79
R_o	0.5

(*v*) Perfect spatial overlap is assumed between the injected beam and the lasting mode. The mode of the injected radiation is matched with one of the cavity mode.
(*vi*) In the case of pulsed injection seeding, the temporal shape of the seed pulse is assumed to be Gaussian.

Under these assumptions, a set of equations is reduced as follows. The upper state population $N(z, t)$, where the optical axis z is measured as shown in Fig. 9, is given by the following formula at $t = 0$:

$$N(z,0) = \frac{\alpha E_{po}}{h\nu_p S} \exp[-\alpha(z - z_1)], \tag{2}$$

where α is the absorption coefficient of the crystal at the pump frequency ν_p, E_{po} is the pump energy, S is the cross section of the laser beam, and z_1 is the position of the surface of the crystal from which the pump light enters.

For the laser photon flux densities with respect to the wavelength λ inside the laser cavity $I_\lambda^{\pm}(z, t)$ ($\pm$ denotes forward and backward direction), the upper-state population density $N(z, t)$, based on the above assumptions, the following rate equations are reduced:

$$\frac{1}{c}\frac{\partial I_\lambda^{\pm}(z,\ t)}{\partial t} + \frac{\partial I_\lambda^{\pm}(z,t)}{\partial z} = \sigma_e(\lambda)N(z,\ t)I_\lambda^{\pm}(z,\ t) + \frac{N(z,\ t)}{\tau}E(\lambda)f, \tag{3}$$

$$\frac{dN}{dt} = -N(z,\ t)\Sigma\{[I_\lambda^{\pm}(z,\ t) + I_\lambda^{-}(z,t)]\sigma_e(\lambda)\} - \frac{N(z,\ t)}{\tau}, \tag{4}$$

where $\sigma_e(\lambda)$ is the stimulated emission cross section with respect to the wavelength λ, c is the speed of light, τ is the fluorescence lifetime, $E(\lambda)$ is the normalized fluorescence intensity, and f is the fraction of spontaneous emission coupled to each mode.

We assumed the laser cavity with the mirror reflectivities of R_o and R_e and a length of L. R_o is the reflectivity of the coupling mirror, R_e is the reflectivity of the end mirror including all of the cavity losses besides R_o. In Fig. 9, the following boundary conditions are used for the simulation:

$$I_\lambda^{+}(0,t) = R_e I_\lambda^{-}(0,t) \quad \text{at } z = 0, \tag{5}$$

$$I_\lambda^{-}(L,\ t) = R_o I_\lambda^{+}(L,\ t) + I_{seed} \quad \text{at } z = L, \tag{6}$$

$$I_{seed} = 0 \quad \text{for } \lambda \neq \lambda_{seed}, \tag{7}$$

$$I_{seed} = I_{seed}(t) \quad \text{for } \lambda = \lambda_{seed}, \tag{8}$$

where $I_{seed}(t)$ is the injection power depending on time t at a particular injection wavelength λ_{seed}.

The output characteristics $I_{\lambda\_out}(t)$ are given by the following equation:

$$I_{\lambda\_out}(t) = (1 - R_o)I_\lambda^{+}(L,t)h\frac{C}{\lambda}S \quad \text{for } \lambda \neq \lambda_{seed}, \tag{9}$$

$$I_{\lambda\_out}(t) = (1 - R_o)(I_\lambda^{+}(L,t) + I_{seed})h\frac{C}{\lambda}S \quad \text{for } \lambda = \lambda_{seed}, \tag{10}$$

where the second term I_{seed}, on the right-hand side of (10), is negligible after the injection seeding is achieved.

These equations are solved numerically using parameters listed in Table 1. Solutions for the differential equations are calculated for 750–850 nm wavelengths at a constant interval of 5 nm and each 5 nm region is subdivided into parts of 0.1 nm. The cavity length is assumed to be 300 nm, and it is subdivided into an integration time step of 0.833 ps.

2.2 Results and discussions

In the first stage, the calculation was carried out for a slave Ti : Sapphire laser oscillator without any injection seeding. The temporal changes of output spectra in free-running condition are shown in Fig. 10; (a) at 5 ns, (b) at 10 ns, (c) at 15 ns, and (d) at 26.4 ns after pumping. At the earlier stage of the laser oscillation, the output spectrum approximately followed that of the fluorescence. At 5 ns, the output spectrum peaked at approximately 78 nm with a width of 70 nm. Subsequently, during build up the spectrum peak shifted towards the longer wavelength, and the narrowing of the spectra is apparent. At 26.4 ns, it peaked at approximately 792 nm with a width of 30 nm. The peak shifting is because of the different peak wavelength for the spectra of the fluorescence and the stimulated emission cross section of the Ti : Sapphire crystal [8].

In the next stage, cw injection power of 30 mW was injected at a wavelength of 790 nm keeping the conditions equal to those used in the first stage. Figure 11 shows output spectra of the slave laser at different instants, i.e., at (a) 5 ns, (b) 10 ns, (c) 15 ns, and (d) 24.4 ns. In this case, the spectrum consisted of a narrow spectrum with a broad background. Both components are increasing with respect to the time, but the broad component is quenched concentrating 97% of the output energy into the injected mode.

Subsequently, a wing injection seeding (case II) was calculated by assuming that the injected radiation has a wavelength away from the maximum gain peak, i.e., at 760 nm. Figure 12 shows cw injection power requirements with respect to the locking efficiency ϕ for both cases I and II. Figure 12 indicates that for case I, approximately 0.4 mW of injection power is sufficient for achieving complete injection seeding, while for case II, approximately 4 mW is necessary to achieve a complete injection seeding.

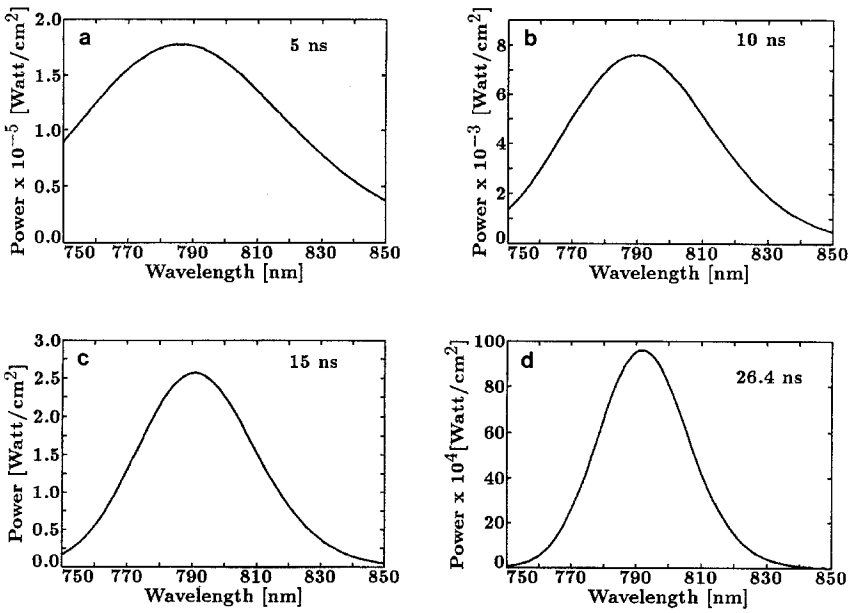

Fig. 10a–d. Simulated spectra of Ti:Sapphire slave laser in free-running condition. **a** Spectrum at 5 ns after pumping, **b** at 10 ns, **c** at 15 ns, **d** at the maximum output, i.e., at 26.4 ns

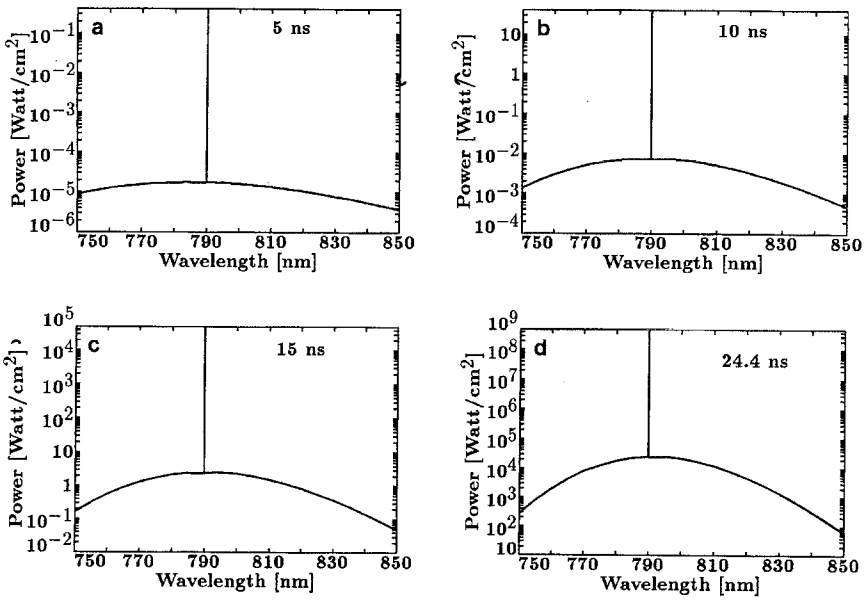

Fig. 11a–d. Simulated spectra of cw injection-seeded Ti:Sapphire slave laser. **a** Spectrum at 5 ns after pumping, **b** at 10 ns, **c** at 15 ns, **d** at the maximum output, i.e., at 24.4 ns

The numerical analysis was further extended for the case of pulsed injection seeding. The effect of different delay ratios on the locking efficiency ϕ was calculated as a function of the injection energy. Figure 13 shows the dependence of the locking efficiency ϕ on the injection energy for different delay ratios. As the delay ratio is changed from 0.25 to 0.65, the injection energy requirements have changed from 3 μJ to 20 mJ exponentially for achieving complete injection seeding.

Based on the numerical simulation of pulsed injection seeding of the slave laser, the effect of delay ratio on the locking efficiency ϕ can be explained as the effect of the mode competition. In the initial stage of the mode competition in the slave laser cavity, the injected mode has high intensity and saturates the gain, while other modes are just beginning to build up from the noise level. As a result, most of the energy stored in the active medium is extracted at the injected frequency. Thus, instead of building up from the noise, the slave laser cavity is filled by photons provided by the injected signal. But when the injection is delayed, the wide gain bandwidth of the laser permits amplification of many modes, and since the energy of these modes increases exponentially with time, the energy requirements increase to achieve the same locking efficiency. Therefore, a complete injection seeding is attained when it is temporally synchronized with the beginning of the slave laser output.

In the case of wing injection seeding the decrease in the locking efficiency ϕ can be explained in a similar way by the effect of mode competition. A lower gain mode, to which injection is done, has to compete with spontaneous emission in the higher gain modes, and it

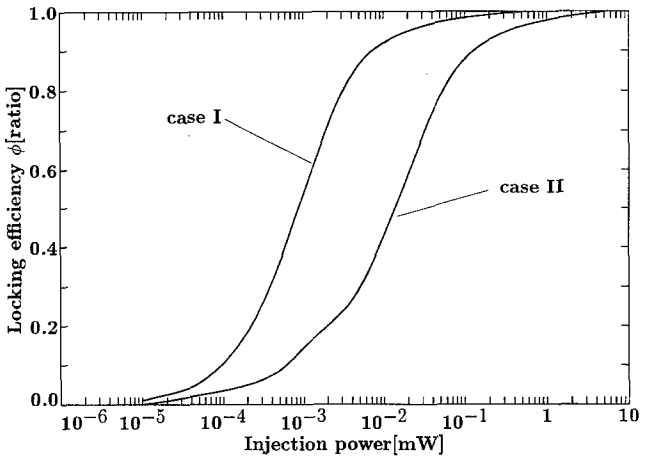

Fig. 12. Theoretically simulated locking efficiency ϕ as a function of cw injection power for different injection-seed conditions. *Case I* is for injection-seed wavelength of 790 nm and *Case II* is wing injection-seeding operation at a wavelength of 760 nm

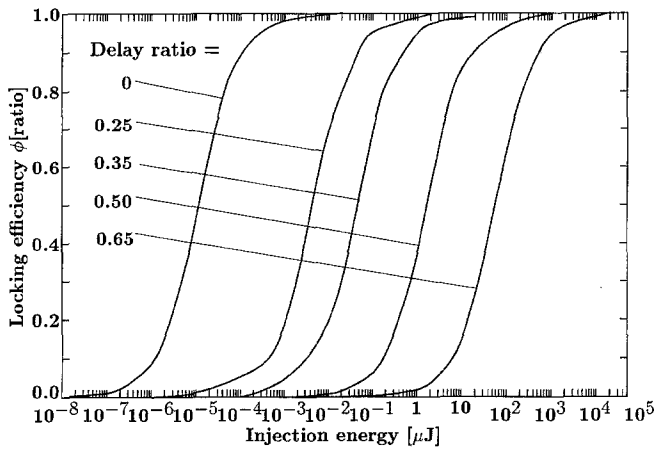

Fig. 13. Theoretically simulated locking efficiency ϕ as a function of injection-seed energy for pulsed injection-seeding operation

cannot build up at a faster rate and requires more injection power to build up. Further, numerical analysis clearly indicates that in case of cw injection only a few tens of μW of injection power was sufficient, while experimental requirements were far above the predicted. This can be explained in terms of longitudinal and spatial mode matching between the slave and the master lasers. Since a perfect spatial mode matching is assumed in the numerical simulation, a higher injection power was required due to imperfectness in the mode matching during the experiment.

3 Conclusions

We report efficient injection seeding of the pulsed Ti:Sapphire laser both with pulsed and cw laser injection seeding. In case of pulsed injection, nearly 100% locking efficiency was obtained with an injection energy of less than 10 μJ, but the performances critically depended on the timing of the injection pulse. In case of cw injection, the spectral width of 0.01 cm^{-1} was obtained with the locking efficiency of 83% at an injected power of 0.73 mW, using a single-mode cw diode laser as an injection source. It was confirmed that the spectral width was as narrow as that of the cw master laser. Experimental characteristics of pulsed and cw injection seeding were explained well by the numerical simulation with spectro-temporal rate equations.

Further, these techniques can permit the development of narrow-band pulsed Ti:Sapphire laser sources that are tunable over much of the near IR, and nonlinear processes can expand the tunable region to IR, visible, and UV.

Acknowledgements. We wish to thank Dr. M. Uchiumi and Dr. Y. Oki for their stimulating discussions and Mr. H. Morita for his earlier work regarding Ti:Sapphire straight and ring laser for the experiment.

References

1. T.D. Raymond, A.V. Smith: Opt. Lett. **16**, 33 (1991)
2. C.H. Bair, P. Brockman, R.V. Hess, E.A. Moldin: IEEE J. QE-**24**, 1045 (1988)
3. P. Brockman, C.H. Bair, J.C. Barnes, R.V. Hess, E.V. Browell: Opt. Lett. **11**, 712 (1986)
4. M.R.H. Knowles, C.E. Webb: Opt. Commun. **89**, 493 (1992)
5. Y. Boucher, P. Georges, A. Brun, J.P. Pocholle, M. Papuchon: Tech. Dig. CLEO '94 (1994) p. 124
6. M. Funayama, K. Mukaihara, T. Okada, M. Maeda, N. Tomonaga, J. Izumi, K. Matsuda, Y. Hasegawa: Rev. Laser Eng. **20**, 752 (1992) (in Japanese)
7. U. Ganiel, A. Hardy, D. Treves: IEEE J. QE-**12**, 704 (1976)
8. J.M. Eggleston, L.G. DeShazer, K.W. Kangas: IEEE J. QE-**24**, 1009 (1988)
9. P.F. Moulton: J. Opt. Soc. Am. B **3**, 125 (1986)